Proceeding of the 2004 American Control Conference
Boston, Massachusetts June 30 - July 2, 2004

Control of EMI from Switch-Mode Power Supplies via Multi-Step Optimization

Daniel E. Quevedo and Graham C. Goodwin

School of Electrical Engineering & Computer Science
The University of Newcastle, Callaghan, NSW 2308, Australia
Emails: dquevedo@ieee.org, eegcg@ee.newcastle.edu.au

***Abstract*— This paper shows how a multi-step optimal conversion architecture can be used as a switching technique for switch-mode power supplies. The strategy presented spreads the power spectrum of the switching signal and, thus, reduces peaks in spectra of voltages and currents within the supply. As a consequence, electromagnetic interference emissions can be mitigated in order to comply with regulations.**

I. Introduction

Switch-mode power supplies (SMPSs) are widely used in electronics equipment, such as computers, which use DC-voltages that need to be provided by the AC mains network. SMPSs are preferred to their linear counterparts mainly due to their reduced size, weight and high power efficiency. These advantages are a consequence of the fact that in an SMPS, power semiconductor switches, such as MOSFETs, are used to synthesize the desired DC voltage levels. The books [1]–[3] constitute general references to SMPSs.

A drawback of using SMPSs resides in the fact that, due to their switching nature, harmonic currents are injected into the AC mains and ground connection. Also, electromagnetic noise is radiated, see also [4]–[8]. This electromagnetic interference (EMI) emission problem may affect the SMPS itself and also interfere with other electronics equipment. This issue becomes especially relevant at high switching frequencies (which are necessary in order to achieve low ripple in the output voltage) and is magnified if many SMPSs are connected to the same supply network. This has lead to a significant degradation of line power quality, for instance, in large office buildings.

In order to deal with the electromagnetic pollution problem, regulations, such as those of the FCC (in the USA) or the VDE (in the EU), have been elaborated, see e.g. [6]. These limit the maximum levels of energy radiated and of the harmonic currents that the equipment is allowed to contaminate the associated supply network. The standards give rise to specifications which are to be satisfied when electronics equipment is to be marketed. In particular, EMI spectra need to be shaped so that large concentrations of energy at discrete frequencies are avoided.

One way to mitigate the EMI problem resides in improving shielding, input filters and isolation of signal coupling paths, see e.g. [2], [3], [5], [8]. These hardware-based methods add to the complexity, size, weight and cost of the power supply. Thus, it may be more convenient to reduce EMI emissions directly at the source. This can be accomplished by careful design of the switching methods of the power device, where one can make use of ever increasing capabilities of DSP hardware. It turns out that EMI emission levels of an SMPS can be predicted by inspecting the spectrum of the switching signal. As a consequence, mitigation of EMI via careful design of the switching strategy has attracted significant research, see e.g. [9]–[13].

Conventional switching strategies for SMPSs utilize periodic Pulse-Width-Modulation (PWM) and yield purely discrete spectra, see e.g. [14]. Thus, this strategy is generally not a good choice if EMI specifications are to be met. In order to broaden signal spectra and reduce harmonic peaks, modified PWM schemes, such as *programmed PWM* [9] and *frequency modulated PWM* [10] have been proposed. Another possibility lies in utilizing randomized PWM schemes, where a nominal PWM switching function is dithered in various ways, see e.g. [11], [12], [15]. Unfortunately, in these methodologies the mitigation of harmonic peaks is usually achieved only at the expense of increased output voltage ripple and this precludes the use of these strategies in SMPSs where tight voltage regulation is sought [14].

By realizing that switching in an SMPS can be regarded as a particular analog-to-digital conversion problem with a 1-bit output, in [13] strategies based upon $\Sigma\Delta$-Modulation have been developed. $\Sigma\Delta$-Modulation has been adopted in many analog-to-digital conversion applications, see e.g. [16]. In the context of SMPSs, [13] illustrates how the most common Single-Loop $\Sigma\Delta$-Modulator does not reduce peak spectra sufficiently for EMI mitigation. Consequently, they propose to deploy either a dithered architecture or a Double-Loop $\Sigma\Delta$-Modulator. We suggest that the latter may be more useful since it is a full-digital approach with constant sampling frequency which does not require any exogenous random signals.

In the present work, we will show how the *Multi-Step Optimal Converter* (MSOC) developed by us in an analog-to-digital conversion setting [17] can be used to provide the switching signal of an SMPS. The MSOC utilizes concepts arising from our work on Predictive Control with finite set constraints, see e.g. [18] and extends our earlier results documented in [19], [20]. It also encompasses general $\Sigma\Delta$-Modulation and, in particular, the modulators used

0-7803-8335-4/04/$17.00 ©2004 AACC

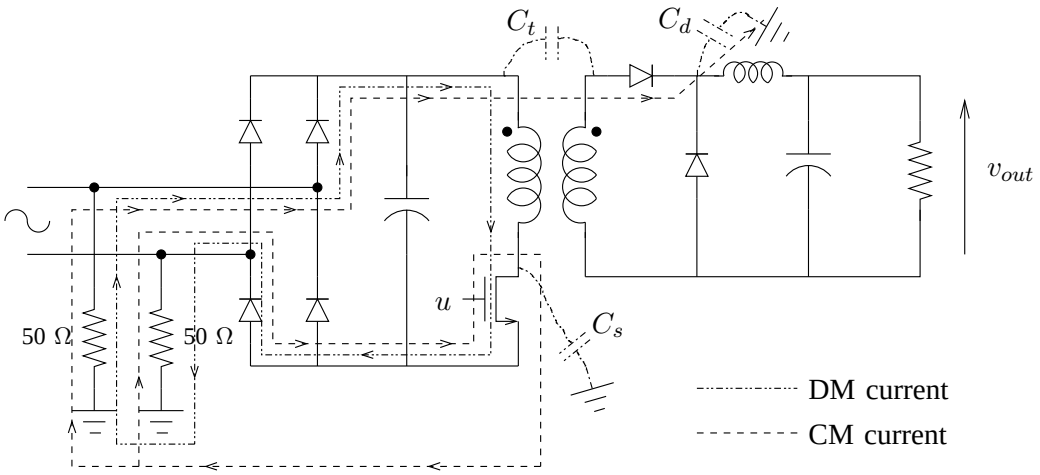

Fig. 1. Conducted EMI emissions in an SMPS.

in [13], as special cases. As will be apparent, the MSOC outperforms these other schemes in relation to suppressing spectral peaks and, thus, constitutes an alternative for EMI mitigation. Note that related ideas were very recently presented orally in [21].

The remainder of the paper is organized as follows: Section II presents the SMPS architecture under study and emphasizes some aspects related to EMI. Section III briefly presents the MSOC and some of its properties. Simulation studies are included in Section IV. Section V draws conclusions.

II. Switch-Mode Power Supplies and Electromagnetic Interference

Fig. 1 shows a circuit diagram for an SMPS forward converter topology analyzed e.g. in [1], [2], [10], [13]. As can be seen in the figure, at the primary side of the transformer, this architecture contains an input bridge diode rectifier with a bulk capacitor. The rectified voltage is fed to a high frequency inverter which is controlled by the solid state switch. At the secondary side, a rectifier diode and a free wheeling diode direct the current to the LC-filter and the (resistive) load.

The main purpose of an SMPS is to deliver a voltage v_{out} to the load. This voltage should be approximately equal to some prescribed (generally constant) value. Towards that goal, the gate signal u needs to chosen carefully. It is a switching signal, which, at any given time, adopts only one of two values corresponding to the *on* and *off* state of the switch. Regulation of v_{out} is equivalent to choosing u such as to approximate a reference signal. This signal can be fixed off-line, yielding an unregulated power supply. The reference signal for u can also be calculated via feedback from the load, thus allowing for compensation against line- and load- variations. In this case, a regulated (controlled) power supply is obtained.

Due to the switching action inherent in an SMPS, high di/dt and dv/dt values can be observed. These, in turn, generate time-varying electromagnetic fields and result in high-frequency *radiated*- and *conducted*- EMI emissions. Radiated EMI is propagated as E and H waves and can be measured with an antenna or a probe. On the other hand, conducted EMI manifests itself on supply lines and interconnecting wires. It is propagated via direct metal-to-metal coupling or also via (parasitic) inductive and capacitive effects. Depending upon whether it affects the AC supply lines or flows in the ground, conducted EMI can be further divided into *differential mode* (DM) and *common mode* (CM) emissions, see also [4]–[8].

In order to show the main paths of conducted EMI emissions, we have included parasitic capacitances in the circuit of Fig. 1, where the capacitance effects between the chassis and the switch and the chassis and the diodes of the secondary side of the supply are denoted as C_s and C_d, respectively. The inter-winding capacitance of the transformer is denoted as C_t. The two 50 Ω resistors included at the primary side correspond to the noise-frequency equivalent of a *Line Impedance Stabilizing Network*, see e.g. [2], commonly used to measure conducted EMI. Generally one of these resistors is the input impedance of a spectrum analyzer. Its voltage is defined as the conducted EMI emission of the circuit. It can be seen, that conducted EMI emissions are related to component selection and physical layout of the SMPS, which for instance, determine the values of the parasitic capacitances. Thus, the EMI compliance problem can be addressed by careful design of components, their distribution and the inclusion of additional filters and shielding devices, as described e.g. in [2], [3], [5], [8].

Alternatively, one can treat EMI emissions directly at the generating source: the gate signal u, which determines the switching of the transistor. Indeed, spectral characteristics of conducted and radiated EMI emissions, which are of fundamental interest for compliance with EMI standards, are closely related with the spectrum of u, see e.g. [9]–[13].

III. A Switching Strategy Which Reduces EMI

As already mentioned, EMI regulations limit the size of the peaks in the EMI emission spectra. Thus, it is useful to limit peaks of the spectrum of the switching signal u, i.e. to spread its energy. This can be achieved by designing u via some optimality criterion. With that goal in mind, we will utilize the *multi-step-optimal* analog-to-digital conversion scheme proposed by us in [17]. The method is an example of *pulse density modulation*, where the number of pulses per unit time depends upon the magnitude of the input.

A. Frequency Selective Noise Suppression

In accordance with contemporary DSP techniques, we adopt a discrete-time framework. In particular, the switching signal u is updated at a fixed sampling frequency, f_s. Between sampling instants, a zero-order-hold is used, i.e. u is kept constant [22]. To keep notation simple, we will denote the samples as $u(\ell)$, $\ell \in \mathbb{N}$. These values are restricted to belong to a binary set, which we will normalize to

$$\mathbb{U} \triangleq \{0, 1\}. \tag{1}$$

With this, the digital value $+1$ turns the semiconductor switch *on* (i.e. it conducts) and the value 0 turns the current flow through the switch off. (Note that u needs to be conditioned in order to be able to drive a power switch, see e.g. [13].)

In order to incorporate frequency weighting into the switching problem, consider a stable linear time-invariant single-input single-output discrete-time filter W, where:

$$W(z) = D + C(zI - A)^{-1}B.$$

Furthermore, define the pre-filtered reference signal

$$a \triangleq Hr,$$

where r is the discrete time reference for the signal u and H is a given discrete-time filter.

The *filtered distortion* signal e is defined as:

$$e \triangleq W(a - u)$$

and can also be characterized as the output of the state-space system:

$$\begin{aligned} x(\ell + 1) &= Ax(\ell) + B(a(\ell) - u(\ell)) \\ e(\ell) &= Cx(\ell) + D(a(\ell) - u(\ell)). \end{aligned} \tag{2}$$

With this as background, the SMPS modulation problem can be stated as one of choosing the binary stream u so as to minimize some measure of e. It is intuitively clear that such a strategy allows one to manipulate the spectrum of u by choosing the filters W and H. Indeed, u will approximate the filtered signal a and the distortion $a-u$ will tend to have a spectrum similar to that of the inverse of W. Thus, careful tuning of H and, especially, of W can be used in order to manipulate the EMI of SMPSs in different frequency bands.

For convenience, we choose at time $\ell = k$, the following measure defined over a finite and fixed horizon $N \in \mathbb{N}$:[1]

$$V_N(\vec{u}(k)) \triangleq \|x'(k+N)\|_P^2 + \sum_{\ell=k}^{k+N-1} (e'(\ell))^2, \tag{3}$$

where P is a given positive semidefinite matrix and the vector

$$\vec{u}(k) \triangleq \begin{bmatrix} u'(k) & u'(k+1) & \dots & u'(k+N-1) \end{bmatrix}^T$$

contains the decision variables. The measure (3) examines predictions of the filtered distortion e and the *final* state $x(k+N)$ in (2). These predicted trajectories are formed as:

$$\begin{aligned} x'(\ell + 1) &= Ax'(\ell) + B(a(\ell) - u'(\ell)), \\ e'(\ell) &= Cx'(\ell) + D(a(\ell) - u'(\ell)), \end{aligned}$$

where $\ell = k, k+1, \dots, k+N-1$ and with initial condition:

$$x'(k) = x(k).$$

Note that, given past values of u and a, the state $x(k)$ can be computed exactly from (2).

Obtaining u via minimization of V_N can be regarded as a particular predictive control problem with *plant* W and *controlled input* u. The distinguishing aspect lies in the fact that, as stated above, at each sampling instant, $u(\ell)$ is restricted to belong to the binary set $\mathbb{U}$ defined in (1). This constraint puts the problem into the framework of so-called finite-set constrained-, or *quantized*-predictive control, see [18]. (Alternative finite-set constrained control schemes can be found e.g. in [23], [24].)

B. The Multi-Step-Optimal Converter

In [17] (see also previous work in [19], [20]) we presented the *Multi-Step-Optimal Converter* (MSOC) based upon the optimality idea described above. The MSOC was developed in an analog-to-digital conversion setting. As will be apparent, this scheme can also be utilized for the SMPS EMI mitigation problem under study here.

The MSOC implements the minimizer to the cost function (3) in a receding horizon fashion, i.e. at each sampling instant, $\ell = k$, the output of the converter is set equal to:

$$u(k) = \begin{bmatrix} 1 & 0 & \dots & 0 \end{bmatrix} \arg \min_{\vec{u}(k) \in \mathbb{U}^N} V_N(\vec{u}(k)), \tag{4}$$

where $\mathbb{U}^N \subset \mathbb{R}^N$ is defined via the Cartesian product:

$$\mathbb{U}^N \triangleq \mathbb{U} \times \dots \times \mathbb{U}.$$

This concept of only utilizing the first element of the optimizing sequence mirrors the approach adopted in *Model Predictive Control* schemes, see e.g. [25]–[27].

The optimization problem (4) is a non-convex combinatorial program. In [17] we showed that its solution can be stated in the following form:

$$u(k) = [1\, 0\, \dots\, 0] \Psi^{-1} q_{\tilde{\mathbb{U}}^N} \big(\mathcal{W}(z) H(z) r(k) - \mathcal{F}(z) u(k) \big), \tag{5}$$

[1] $\|x\|_P^2$ denotes the quadratic form $x^T P x$, where x is any vector and P is a matrix.

where $\Psi \in \mathbb{R}^{N\times N}$; $\mathcal{W}(z)$ and $\mathcal{F}(z)$ are matrix transfer functions having 1 input and N outputs, and $q_{\widetilde{\mathbb{U}}^N}(\cdot)$ is a vector quantizer, see the Appendix. This result allows us to characterize the MSOC as the closed loop depicted in Fig. 2.

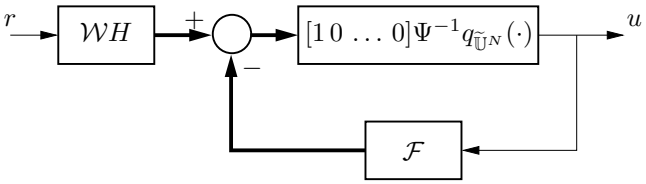

Fig. 2. Implementation of the MSOC as a feedback loop. Thick lines denote vector-signal paths.

C. Properties of the MSOC

The architecture of Fig. 2 bears similarities to a $\Sigma\Delta$-Modulation loop. Indeed, in the special case of a unitary horizon, $N = 1$ in (3) and no terminal state weighting ($P = 0$), the MSOC reduces to a general $\Sigma\Delta$-Modulator as presented e.g. in [16].

In particular, if H and W are chosen as:

$$W(z) = \frac{z^2}{(z-1)^2}, \quad H(z) = z^{-1}, \tag{6}$$

then the *Double-Loop* $\Sigma\Delta$-Modulator is obtained. This scheme has been proposed in [13] for mitigating EMI emissions.

The MSOC has several advantages when compared to $\Sigma\Delta$-Modulation or to PWM. One of these advantages is related to the suppression of limit cycles. It is well known that the use of PWM and $\Sigma\Delta$-Modulation may give rise to a periodic signal u yielding large energy concentrations at discrete frequencies, see e.g. [28]–[34]. As a consequence, when these strategies are deployed, additional expensive hardware such as filters and shielding need to be included in the SMPS in order to comply with EMI specifications. Although randomized strategies may reduce EMI peaks, see e.g. [11], [13], the incorporation of exogenous noise will often introduce additional low-frequency ripple in the output voltage and is thus undesirable in SMPSs with tight voltage regulation specifications, see [14].

Fortunately, in case of the MSOC, spectral peaks can be mitigated without having to use a dither signal. As in the case of Model Predictive Control schemes, see e.g. [26], the role of the matrix P is crucial in establishing stability. For example, we quote the following result from our earlier work described in [17]:

Theorem 1: Suppose that the reference r is such that $r(\ell) \in \mathbb{U}, \forall \ell \geq k$. Then, if P is chosen as the positive definite solution of the Lyapunov Equation

$$A^T P A + C^T C = P, \tag{7}$$

then $e(\ell) \to 0$, as $\ell \to \infty$.

It should be emphasized here that, although this result is of significance only for a restricted class of references, simulation studies, such as those included in Section IV (see also in [17]), indicate that setting P as the *stabilizing* value given in (7) is, in general, a good choice in order to suppress limit cycles and, thus, to reduce peaks in the spectrum of u.

In summary, the MSOC encompasses $\Sigma\Delta$-Modulation in a more general framework. The incorporation of a final state weighting and a horizon N, which can be larger than 1, gives more degrees of freedom in the MSOC design. In general, larger horizons will yield improved performance, since more information is taken into account in the switching design process. Moreover, the terminal state weighting term, $\|x'(k+N)\|_P^2$, is useful to guarantee stability-like properties of the strategy. Thus, the MSOC may give better EMI performance than existing schemes.

IV. Simulation Example

As an example, adapted from [13], consider a sampling frequency $f_s = 300$ kHz and constant references, $r = 0.3$ and $r = 0.36$. (If the DC-link is equal to 5 V, then these reference values correspond to load voltages of 1.5 V and 1.8 V, respectively.)

We utilize two MSOCs with filters

$$W(z) = \frac{z^2}{(z-0.99)(z-0.98)}, \quad H(z) = z^{-1}. \tag{8}$$

The first design uses a unitary constraint horizon, $N = 1$ and no terminal state weighting, i.e. $P = 0$.[2] The second design uses $N = 3$ and the stabilizing value for P which solves the Lyapunov Equation (7). For comparison, we also simulated the case of Double-Loop $\Sigma\Delta$-Modulation proposed in [13], which, as stated before, is equivalent to the MSOC with parameters $N = 1$, $P = 0$ and filters given in (6).

Figs. 3 and 4 illustrate the results. They show the periodograms of the gate signal u held constant in between sampling instants. As can be seen, the filter choice given in (8) is beneficial with regards to limiting the concentration of signal power at discrete frequencies, when compared to Double-Loop $\Sigma\Delta$-Modulation. Moreover, choosing a non-unitary horizon and the stabilizing state weighting helps to reduce peaks further. In the cases simulated, the reduction is of the order of 10 dB.

As a consequence, one can expect the EMI emission peaks caused by an SMPS deploying an MSOC to be smaller than those obtained with the more-restrictive $\Sigma\Delta$-Modulation architecture.

V. Conclusions

In this contribution we have shown how the *Multi-Step Optimal Converter* can be utilized as a switching strategy for SMPSs. Its stabilizing properties reduce the concentration of signal energies at discrete frequencies. As

[2]This case is equivalent to a general $\Sigma\Delta$-Modulator, see e.g. [16].

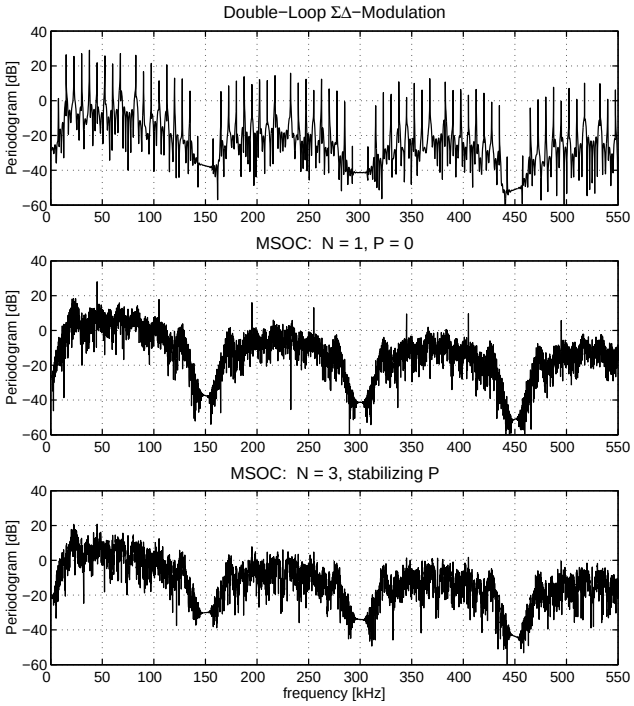

Fig. 3. Periodogram of the sampled data signal u given $r = 0.3$.

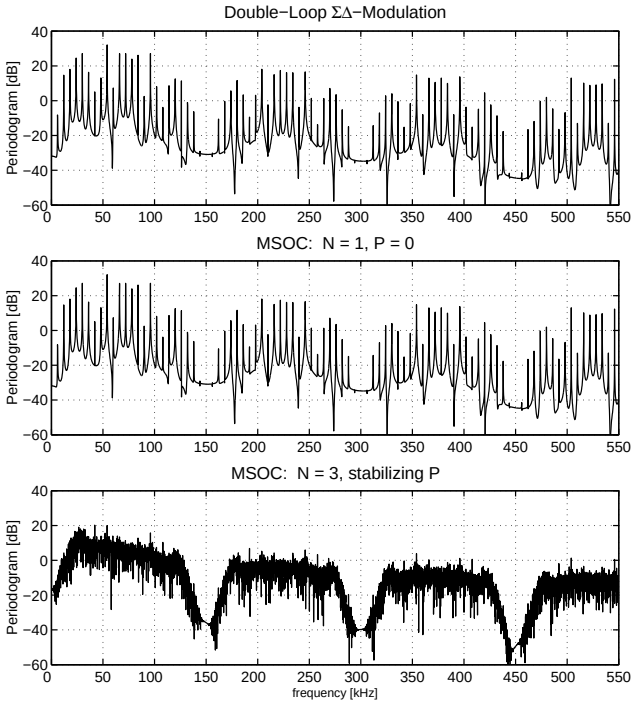

Fig. 4. Periodogram of the sampled data signal u given $r = 0.36$.

a consequence, the MSOC provides a useful alternative for EMI mitigation. It outperforms methods based upon ΣΔ-Modulation.

Planned future work includes the application of this technique to more general power converter architectures, such as those described in [35], [36].

APPENDIX
DEFINITIONS FOR THE RESULT (5)

In (5), the matrix Ψ is square and defined implicitly via

$$\Psi^T\Psi \triangleq \Phi^T\Phi + M^T P M,$$

where:

$$\Phi \triangleq \begin{bmatrix} D & 0 & \dots & 0 \\ CB & D & \ddots & \vdots \\ \vdots & \ddots & \ddots & 0 \\ CA^{N-2}B & \dots & CB & D \end{bmatrix},$$

$$M \triangleq \begin{bmatrix} A^{N-1}B & A^{N-2}B & \dots & AB & B \end{bmatrix}.$$

The matrix transfer functions $\mathcal{W}$ and $\mathcal{F}$ are given by:

$$\mathcal{F}(z) \triangleq \Psi^{-T}(\Phi^T\Gamma + M^T P A^N)(zI - A)^{-1}B,$$

$$\mathcal{W}(z) \triangleq \Psi \begin{bmatrix} 1 & z & \dots & z^{N-1} \end{bmatrix}^T + \mathcal{F}(z),$$

with:

$$\Gamma \triangleq \begin{bmatrix} C & CA & \dots & CA^{N-1} \end{bmatrix}^T.$$

The memoryless nonlinearity $q_{\widetilde{\mathbb{U}}^N}(\cdot)$ is the nearest neighbour (Euclidean) quantizer, which maps its input to the set

$$\widetilde{\mathbb{U}}^N \triangleq \{\widetilde{v}_1,\ \widetilde{v}_2, \dots, \widetilde{v}_r\} \subset \mathbb{R}^N, \text{ with } \widetilde{v}_i = \Psi v_i,\ v_i \in \mathbb{U}^N$$

according to the nearest neighbour rule:

$$q_{\widetilde{\mathbb{U}}^N}(c) = \widetilde{v}_i \in \widetilde{\mathbb{U}}^N \iff \|c - \widetilde{v}_i\| \le \|c - \widetilde{v}_j\|,\ \forall \widetilde{v}_j \in \widetilde{\mathbb{U}}^N.$$

A thorough treatment of vector quantization can be found e.g. in the book [37].

REFERENCES

[1] A. I. Pressman, *Switching Power Supply Design*. New York: McGraw-Hill, second ed., 1998.

[2] K. Billings, *Switchmode Power Supply Handbook*. New York: McGraw-Hill, 1989.

[3] Ö. Ferenczi, *Power Supplies, Part B: Switched-mode Power Supplies*. Amsterdam: Elsevier, 1987.

[4] D. F. Knurek, "Reducing EMI in switch mode power supplies," in *Proc. INTELEC'88*, pp. 411–420, 1988.

[5] M. K. W. Wu and C. K. Tse, "A review of EMI problems in switch mode power supply design," *J. Electric. Electron. Eng. Australia*, vol. 16, no. 3/4, pp. 193–204, 1996.

[6] R. Redl, "Power electronics and electromagnetic compatibility," in *Power Electronics Technology and Applications II* (F. C. Lee, ed.), pp. 275–281, Piscataway, NJ: IEEE Technical Activities Board, 1998.

[7] T. Broom and I. W. Hofsajer, "Some origins and mitigation of conducted common mode EMI in switching converters," in *Proc. IEEE Africon*, pp. 779–784, 2002.

[8] J. B. Wang, "Reduction in conducted EMI noises of a switching power supply after thermal management design," *IEE Proc.–Electr. Power Appl.*, vol. 150, pp. 301–310, May 2003.

[9] A. C. Wang and S. R. Sanders, "Programmed pulsewidth modulated waveforms for electromagnetic interference mitigation in DC–DC converters," *IEEE Trans. Power Electron.*, vol. 8, pp. 596–605, Oct. 1993.

[10] F. Lin and D. Y. Chen, "Reduction of power supply EMI emission by switching frequency modulation," *IEEE Trans. Power Electron.*, vol. 9, pp. 132–137, Jan. 1994.
[11] A. M. Stanković, G. C. Verghese, and D. J. Perreault, "Analysis and synthesis of randomized modulation schemes for power converters," *IEEE Trans. Power Electron.*, vol. 10, pp. 680–693, Nov. 1995.
[12] K. K. Tse, H. S.-H. Chung, S. Y. Hui, and H. C. So, "Analysis and spectral characteristics of a spread-spectrum technique for conducted EMI suppression," *IEEE Trans. Power Electron.*, vol. 15, pp. 399–410, Mar. 2000.
[13] L. Paramesh and A. von Jouanne, "Use of Sigma–Delta modulation to control EMI from switch-mode power supplies," *IEEE Trans. Ind. Electron.*, vol. 48, pp. 111–117, Feb. 2001.
[14] S. Y. Hui, Y. Shrivastava, S. Sathiakumar, K. K. Tse, and H. S.-H. Chung, "A comparision of nondeterministic and deterministic switching methods for DC–DC power converters," *IEEE Trans. Power Electron.*, vol. 13, pp. 1046–1055, Nov. 1998.
[15] Y. Shrivastava, S. Sathiakumar, and S. Y. Hui, "Improved spectral performance of random PWM schemes with weighted switching decision," *IEEE Trans. Power Electron.*, vol. 13, pp. 1038–1045, Nov. 1998.
[16] S. R. Norsworthy, R. Schreier, and G. C. Temes, eds., *Delta–Sigma Data Converters: Theory, Design and Simulation*. Piscataway, N.J.: IEEE Press, 1997.
[17] D. E. Quevedo and G. C. Goodwin, "Multi-step optimal analog-to-digital conversion," Tech. Rep. EE03032, School of Elect. Eng. and Comput. Sci., The Univ. of Newcastle, NSW 2308, Australia, 2003.
[18] D. E. Quevedo, G. C. Goodwin, and J. A. De Doná, "Finite constraint set receding horizon control," *Int. J. Robust Nonlin. Contr.*, vol. 14, pp. 355–377, Mar. 2004.
[19] G. C. Goodwin, D. E. Quevedo, and D. McGrath, "Moving-horizon optimal quantizer for audio signals," *J. Audio Eng. Soc.*, vol. 51, pp. 138–149, Mar. 2003.
[20] D. E. Quevedo and G. C. Goodwin, "Audio quantization from a receding horizon control perspective," in *Proc. Amer. Contr. Conf.*, pp. 4131–4136, 2003.
[21] A. Rantzer and S. Hedlund, "Density and cost in non-linear control." Semi-Plenary Address, European Contr. Conf., Cambridge, UK, Sept. 2003.
[22] K. J. Åström and B. Wittenmark, *Computer controlled systems. Theory and design.* Englewood Cliffs, N.J.: Prentice Hall, second ed., 1990.
[23] A. Bicchi, A. Marigo, and B. Piccoli, "On the reachability of quantized control systems," *IEEE Trans. Automat. Contr.*, vol. 47, pp. 546–562, Apr. 2002.
[24] R. W. Brockett and D. Liberzon, "Quantized feedback stabilization of linear systems," *IEEE Trans. Automat. Contr.*, vol. 45, pp. 1279–1289, July 2000.
[25] J. M. Maciejowski, *Predictive Control with Constraints*. Prentice-Hall, 2002.
[26] D. Q. Mayne, J. B. Rawlings, C. V. Rao, and P. O. M. Scokaert, "Constrained model predictive control: Optimality and stability," *Automatica*, vol. 36, no. 6, pp. 789–814, 2000.
[27] S. J. Qin and T. A. Badgwell, "A survey of industrial model predictive control technology," *Contr. Eng. Pract.*, vol. 11, pp. 733–764, 2003.
[28] M. Rubensson and B. Lennartson, "Global convergence analysis for piecewise linear systems applied to limit cycles in a DC/DC converter," in *Proc. Amer. Contr. Conf.*, pp. 1272–1277, 2002.
[29] M. di Bernardo, F. Garofalo, L. Iannelli, and F. Vasca, "Bifurcations in picewise-smooth feedback systems," *Int. J. Contr.*, vol. 75, no. 16/17, pp. 1243–1259, 2002.
[30] O. Woywode, J. Weber, H. Güldner, A. Baranovski, and W. Schwarz, "Bifurcation and statistical analysis of DC–DC converers," *IEEE Trans. Circuits Syst. I*, vol. 50, pp. 1072–1080, Aug. 2003.
[31] Z. T. Zhusubaliyev, E. A. Soukhoterin, and E. Mosekilde, "Quasi-periodicity and border-collision bifurcations in a DC–DC converter with pulsewidth modulation," *IEEE Trans. Circuits Syst. I*, vol. 50, pp. 1047–1057, Aug. 2003.
[32] Z. T. Zhusubaliyev and E. Mosekilde, *Bifurcations and Chaos in Piecewise-Smooth Dynamical Systems*, vol. 44 of *Nonlinear Science, Series A*. Singapore: World Scientific Publishing Co., 2003.
[33] P. J. Ramadge, "On the periodicity of symbolic observations of piecewise smooth discrete-time systems," *IEEE Trans. Automat. Contr.*, vol. 35, pp. 807–813, July 1990.
[34] O. Feely, "A tutorial introduction to non-linear dynamics and chaos and their application to Sigma-Delta modulators," *Int. J. Circuit Theory Appl.*, vol. 25, pp. 347–367, 1997.
[35] J. Rodríquez, J.-S. Lai, and F. Z. Peng, "Multilevel inverters: A survey of topologies, controls, and applications," *IEEE Trans. Ind. Electron.*, vol. 49, pp. 724–738, Aug. 2002.
[36] H. Akaki, "Large static converters for industry and utility operations," *Proc. IEEE*, vol. 89, pp. 976–983, June 2001.
[37] A. Gersho and R. M. Gray, *Vector Quantization and Signal Compression*. Kluwer Academic, 1992.